Melting of polydisperse colloidal crystals in nonequilibrium

H. Löwen and G. P. Hoffmann
Institut für Theoretische Physik II, Heinrich-Heine-Universität Düsseldorf, Universitätsstraße 1, D-40225 Düsseldorf, Germany
(Received 23 March 1999)

The influence of a time-dependent oscillatory external field on the melting transition of a polydisperse colloidal crystal is examined by theory and computer simulation. In a monodisperse crystal the field just induces an overall dynamical mode which does not affect the melting line. For a polydisperse sample, on the other hand, the field shifts the melting line towards smaller temperatures. Combining a solid cell approach and a Lindemann criterion in nonequilibrium, a simple theory is presented showing that the temperature shift scales with the square of the relative polydispersity. The theory is in reasonable agreement with nonequilibrium Brownian dynamics computer simulations. [S1063-651X(99)11908-1]

PACS number(s): 82.70.Dd, 64.70.Dv

I. INTRODUCTION

While by now equilibrium melting and freezing transitions are microscopically well understood within theory, experiment, and computer simulation [1,2], much less is known about these phase transformations away from equilibrium. Rapid temperature quenches, for instance, are known to produce metastable thermodynamic phases [3,4]. Another nonequilibrium situation is induced by an external time-dependent oscillatory field. Soft matter materials such as colloidal suspensions are excellent model systems to study equilibrium phase transition [5,2,6] and are also vulnerable to small external perturbations. They thus represent ideal samples for which the influence of external time-dependent oscillatory fields can be studied quantitatively.

In this paper we study the influence of an external oscillatory field on the melting transition of colloidal crystals. As a model, we describe the motion of the colloidal particles by completely overdamped Brownian motion under the influence of an external time-dependent but space-independent force. Such a coupling can be realized in quite different experimental setups [6]: Both electric [7] or laser-optical [8] external fields can be superimposed to the colloidal sample. They act as an external force since the material of the colloidal particles possesses another dielectric constant other than the solvent. For magnetic colloids an alternating external homogeneous magnetic field results in the same external coupling [9]. A third realization are colloids under shear. In contrast to the typical case of linear shear flow where many experimental [10], theoretical [11], and computer simulation [12] studies are available, we focus here on oscillatory shear fields which were also investigated by experiments [13,14] and simulations [15]. Our model is identical to an oscillatory shear situation in the limit of small shear rates. As we shall show, polydispersity becomes crucial for the shift of the nonequilibrium melting transition in this limit. Finally, the colloidal sedimentation problem in a constant gravitational field is recovered as a special case in our model by setting the frequency of the external field to zero. Regarding the latter situation, Batchelor and co-workers [16] already emphasized that polydispersity has a significant effect on the sedimentation velocity (see also Ref. [17]).

In this work, we show that an external oscillating field shifts the solid melting line towards lower temperatures with respect to the field-free equilibrium case. In order to do so, we have performed extensive nonequilibrium Brownian dynamics (BD) computer simulations. We also propose a simple Lindemann rule of melting suitably generalized to nonequilibrium which is confirmed by our simulations. Concrete results for the melting line are obtained with the help of a cell model for charge-polydisperse colloidal suspensions interacting via an effective Yukawa potential. The trends as obtained from the theory are in reasonable agreement with the BD simulations. One of our main results is that the shift of the solid melting line scales with the square of the relative polydispersity of the colloidal sample. Since melting curves can be measured precisely by light scattering techniques [18], our result may facilitate a direct measurement of polydispersity which is normally seen only indirectly in a smeared structure factor.

This paper is organized as follows: In Sec. II, the model is introduced. Then we describe the generalized Lindemann criterion for a nonequilibrium situation in Sec. III. Our BD simulation techniques are summarized in Sec. IV. Section V is devoted to a discussion of the results and to a comparison of theory and simulation. We finally conclude and state some interesting open questions in Sec. VI.

II. MODEL

We consider N colloidal particles in a volume Ω with a fixed number density $\rho = N/\Omega$. The colloidal suspension is held at fixed temperature T since it is embedded in a bath of microscopic solvent particles of the same temperature. The colloidal particles i and j are interacting via an effective pair potential $V_{ij}(r) = Z_i Z_j V_0(r)$, where r is the interparticle distance. Here we have introduced a polydispersity in the effective interaction between the colloidal particles by the intrinsic particle property Z_i $(Z_i > 0)$. In fact, this particle property is a random variable Z which is distributed according to a normalized distribution function $p(Z)$ with a mean value

$$\overline{Z} = \int_0^\infty dZ\, Z p(Z) \tag{1}$$

and a relative polydispersity

$$p_Z = \sqrt{\overline{Z^2}/\overline{Z}^2 - 1}. \tag{2}$$

Typical examples are charge- and size-polydisperse colloids [19,20] where

$$Z_i = Q_i \exp(\kappa\sigma_i/2)/(1+\kappa\sigma_i/2) \tag{3}$$

is the effective charge (with Q_i and σ_i denoting the bare charge and diameter of the ith particle) and $V_0(r) \propto \exp(-\kappa r)/r$ has a Yukawa form (with κ denoting the inverse Debye screening length).

The dynamics of the colloids is assumed to be Brownian. Hydrodynamics interactions are neglected which is a safe approximation if the colloidal volume fraction is small. Under these conditions any energy transferred onto the colloidal particles via the external field is immediately damped by the solvent friction. The friction constant $\gamma_i = 3\pi\eta\sigma_i$ with η denoting the shear viscosity of the solvent) is directly proportional to the polydispersity in size, which can be extracted from a normalized size-distribution function $p(\sigma)$ with a first moment $\overline{\sigma}$ and a relative polydispersity $p_\sigma = \sqrt{\overline{\sigma^2}/\overline{\sigma}^2 - 1}$. Strictly speaking, the distribution function p and the bar have a different meaning here than in Eqs. (1) and (2). We nevertheless keep the same notation since it is clear from the argument which kind of polydispersity and which kind of average is meant.

The external oscillatory force acting on the ith particle is pointing in the z direction and modeled as

$$\vec{F}_i(t) = \vec{e}_z f_i \cos(\omega t) \tag{4}$$

where ω is the external frequency, $\vec{e}_z$ is the unit vector along the z direction, and f_i is the coupling parameter of the ith particle to the external field. The variable $\{f_i\}$ describe a third kind of polydispersity which we call coupling polydispersity. It is characterized by a normalized distribution function $p(f)$ with mean $\overline{f}$ and relative rootvariance $p_f = \sqrt{\overline{f^2}/\overline{f}^2 - 1}$. For charged suspensions in an electric field, $f_i = Q_i E_0$, where E_0 is the amplitude of the effective electric field [21].

Our first important consideration concerns samples which are monodisperse in size and coupling, i.e., $p_\sigma \equiv p_f \equiv 0$. Since all particles feel the same external force, the net effect of the coupling is a trivial dynamical mode

$$\vec{r}_0(t) = \vec{e}_z \overline{f} \sin(\omega t)/3\pi\eta\omega\overline{\sigma}. \tag{5}$$

In fact, the stochastic Langevin equations for the colloidal trajectories $\vec{r}_i(t)$ $(i = 1, \ldots, N)$ read as

$$\gamma_i \frac{d\vec{r}_i}{dt} = -\vec{\nabla}_{\vec{r}_i} \sum_{j \neq i} V_{ij}(|\vec{r}_i - \vec{r}_j|) + \vec{F}_i(t) + \vec{F}_i^{(R)}(t) \tag{6}$$

where the random forces $\vec{F}_i^{(R)}$ describe the kicks of the solvent molecules acting onto the ith colloidal particle. These kicks are Gaussian random numbers with zero mean, $\overline{\vec{F}_i^{(R)}} = 0$, and variance

$$\overline{(\vec{F}_i^{(R)})_\alpha(t)(\vec{F}_j^{(R)})_\beta(t')} = 2k_B T \gamma_i \delta_{\alpha\beta}\delta_{ij}\delta(t-t'). \tag{7}$$

The subscripts α and β stand for the three Cartesian components and $k_B T$ is the thermal energy. The Langevin equations (6) can be rewritten in terms of new reduced trajectories $\tilde{\vec{r}}_i(t) \equiv \vec{r}_i(t) - \vec{r}_0(t)$ such that the transformed equations have the same form as the original ones in the field-free case [22]. This immediately implies that any structural correlations of the colloidal particles are unaffected by the field. In particular the solid melting line does not depend on the external field strength $\overline{f}$. However, the situation is different if the size or coupling polydispersity in nonvanishing. This will be explored theoretically in the next section.

III. LINDEMANN CRITERION IN NONEQUILIBRIUM

A. General outline of the theory

Let us assume that all polydispersities are small. We further adopt the picture of a harmonic solid using a solid cell model with fixed neighbors located at the lattice positions $\{\vec{R}_j\}$. On average, these particles constitute a cage potential for which we assume no occupation correlations, i.e., we approximate in Eq. (6)

$$\sum_{j \neq i} V_{ij}(|\vec{r}_i - \vec{r}_j|) \approx \sum_{j \neq i} \overline{Z} Z_i V_0(|\vec{R}_j - \vec{r}_i|) \approx \overline{V} + \tfrac{1}{2} Z_i K (\vec{r}_i - \vec{R}_i)^2. \tag{8}$$

Here we assumed cubic crystal symmetry such that the harmonic picture becomes isotropic. $\overline{V}$ is an irrelevant additive constant. The effective ''spring constant''

$$K = \sum_{\vec{R}_j \neq 0} \frac{\overline{Z}}{3} [V_0''(R_j) - 2V_0'(R_j)/R_j] \tag{9}$$

depends (via the lattice constant) on the colloidal density ρ. Equation (9) assumes that one lattice point is in the origin; $V_0'(r)$ and $V_0''(r)$ denote the first and second derivative of V_0 with respect to r. Within these approximations the stochastic Langevin equations describe a driven Brownian harmonic oscillator. As a side step we remark that this picture of the colloidal crystal has been directly proved by dynamic light scattering experiments in equilibrium [23]. Transforming again onto reduced trajectories $\tilde{\vec{r}}_i(t) = \vec{r}_i(t) - \vec{r}_0(t)$ and onto reduced lattice positions $\tilde{\vec{R}}_j(t) = \vec{R}_j(t) - \vec{r}_0(t)$, one can readily calculate the polydispersity average of the reduced mean-square displacement. If the frequency ω is comparable to a typical inverse time scale of the colloidal motion, it makes sense to also perform a time average. The result for the full averaged mean-square displacement is

$$\langle \tilde{\vec{r}}_i^2 \rangle = \frac{3k_B T}{K\overline{Z}}(1 + p_Z^2) + \frac{1}{2}\frac{\overline{f^2}}{\Gamma^2 + \omega^2} \times \left(p_f^2 + p_\sigma^2 - 2\overline{(f_i/\overline{f} - 1)(\sigma_i/\overline{\sigma} - 1)} \right) \tag{10}$$

with $\Gamma = K\overline{Z}/3\pi\eta\overline{\sigma}$. The right-hand-side of Eq. (10) consists of five terms. For the equilibrium case (i.e., zero external field, $\overline{f} \equiv 0$), only the first two terms are relevant: The aver-

aged mean-square displacement is increasing with increasing polydispersity and the leading correction is quadratic in p_Z. Furthermore, if there is no correlation between the two distributions in f and σ, the last term vanishes. Size and coupling polydispersity both enhance the mean-square displacement and the leading order scales again with the square of p_f and p_σ.

To access the melting curve we now use the Lindemann rule [24] in a generalized sense. It states that a solid melts if its root-mean-square displacement is roughly 15% of the mean distance $a=\rho^{-1/3}$ between the particles [25]. We postulate that this rule is also valid in our nonequilibrium situation. In fact, a high-frequency rattling field may be seen as an increase of the ''effective'' system temperature thus justifying a quasiequilibrium treatment. Hence the solid melting curve is obtained by

$$\frac{\sqrt{\langle \vec{r}_i^{\,2} \rangle}}{a} = L_0, \tag{11}$$

where L_0 is the Lindemann parameter for the associated monodisperse system in equilibrium. This relation together with Eq. (10) determines the location of the solid melting line.

B. Application of the theory to an equilibrium situation

Let us now check our theory in an equilibrium situation by comparing it to simulation data for the melting line. We discuss both monodisperse and polydisperse systems for hard sphere and Yukawa interactions.

For a monodisperse hard-sphere system, the Lindemann parameter at melting of the face-centered cube (fcc) crystal lattice is $L_0=0.13$ [26]. Our cell model gives $L_0=0.11$ in good agreement with the simulation. In evaluating our theory, we have taken the solid melting density from computer simulation.

The cell theory, however, underestimates L_0 if the interactions become softer. Detailed computer simulations of the melting line of a Yukawa solid are available [27–29,25]. The associated solid lattice structure is fcc for hard interactions (i.e., for $\kappa\rho^{-1/3}>4$) and body-centered-cubic (bcc) for soft interactions (i.e., for $\kappa\rho^{-1/3}<4$). From the simulations, it is known that the Lindemann parameter along the melting curve increases with decreasing $\kappa\rho^{-1/3}$ from the hard sphere value 0.129 ($\kappa\rho^{-1/3}\to\infty$) to the plasma value 0.19 ($\kappa\rho^{-1/3}=0$). Our theory, evaluated at the solid melting curve, yields $L_0=0.09-0.10$ which is significantly lower than the simulation data. Hence the solid cell model becomes less reliable for softer interactions.

We now turn to polydisperse systems in equilibrium. In fact recent computer simulations on size- [30] and charge- [31] polydisperse colloids indicate that the Lindemann rule is valid with polydispersity. As far as actual numbers for the melting line are concerned, there are only few computer simulation data available. An accurate solid melting curve was obtained recently using thermodynamic integration for a size-polydisperse hard-sphere fcc crystal by Bolhuis and Kofke [32]. The melting density grows with increasing polydispersity and scales with p_σ^2 for small p_σ consistent with our theory. If one constructs a similar cage-cell theory [33,34] for the size-polydisperse hard-sphere crystal, the application of the criterion (11) yields perfect agreement with the simulation data up to a relative size polydispersity of 5%. The same is true if one applies the Lindemann criterion (11) for a charge-polydisperse case. Here one can reasonably re-

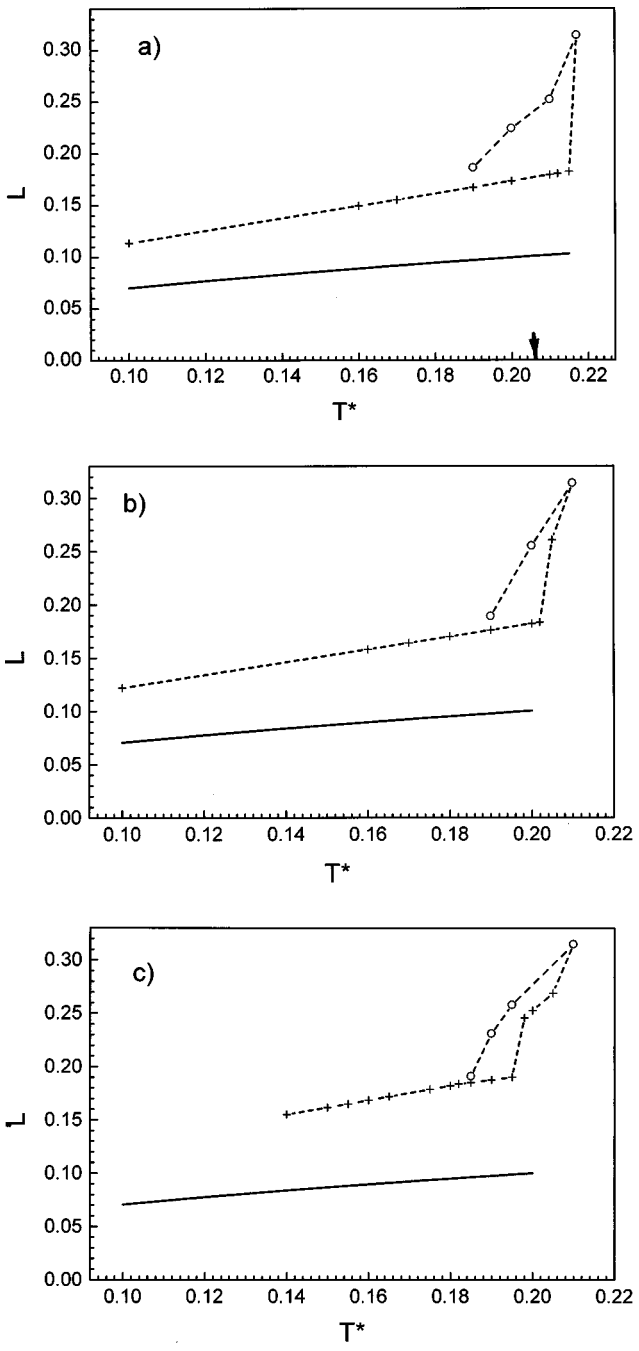

FIG. 1. Averaged Lindemann parameter L vs reduced temperature T^*. The solid line is the theoretical result using the cell model. The dotted line is from computer simulation. The crosses show a heating situation, while the open circles correspond to a cooling situation. (a) Equilibrium situation of a monodisperse system, $p_Z=0$. Here the exact melting temperature as known from Ref. [28] is indicated by the arrow; the parameter λ is equal to 5.8. (b) Equilibrium situation with polydispersity $p_Z=0.1$, $\lambda=5.8$ and $E_0/k_BT=0$. (c) Nonequilibrium situation with $p_Z=0.1$, $\lambda=4.8$, $\omega\tau=570$, $E_0/k_BT=100$.

produce the simulation data of Ref. [31] up to a relative charge polydispersity of 20%. As for further full quantitative comparison between theory and simulation, we refer to Figs. 1(a) and 1(b) and to our discussion in Sec. V.

IV. BROWNIAN DYNAMICS COMPUTER SIMULATIONS IN NONEQUILIBRIUM

Our Brownian dynamics (BD) code is very similar to an equilibrium simulation of charge-polydisperse colloids [19]. We put $N=864$ particles into a cubic cell of length l with periodic boundary conditions. The colloidal number density is $\rho=N/l^3$. The particles interact via an effective Yukawa pair potential

$$V_{ij}(r)=Z_iZ_jU_0\exp(-\kappa r)/\kappa r, \tag{12}$$

where U_0 sets the energy scale. The (dimensionless) charges Z_i are drawn from a rectangular distribution around a mean value Z which is set to 1 without loss of generality:

$$p(Z)=\begin{cases} 1/\sqrt{12}p_Z & \text{for } |Z-1|<\sqrt{3}p_Z \\ 0 & \text{elsewhere.} \end{cases} \tag{13}$$

The width of the distribution is fixed by the prescribed polydispersity p_Z. All particles have the same diameter σ. Consequently, their friction constant γ is also the same. The coupling polydispersity is taken to be proportional to the charge polydispersity, i.e., $f_i=E_0Z_i$, where E_0 measures the amplitude of the oscillating field. The direction of the external force is always along an edge of the simulation box. We remark that in equilibrium, any thermodynamic quantity only depends on the two parameters $\lambda=\kappa\rho^{-1/3}\equiv\kappa a$ and $T^*=k_BT\exp(\lambda)/U_0$ [28]. Of course, this is no longer true in nonequilibrium. In a steady state, the external field introduces two additional parameters: the field amplitude gives a further energy scale and the frequency sets an additional time scale.

Our starting configuration was a fcc lattice which was randomly occupied by particles of different charge. For $\lambda=5.8$, as chosen throughout our simulations, this structure is the thermodynamically stable one, at least for small polydispersities [28]. We have checked explicitly by taking different random occupations, that our results were not affected by the initial occupation. The Langevin equations of motion including the shaking external field were numerically solved using a finite time step Δt and the technique of Ermak [35,36]. The Brownian time scale is set by $\tau=\gamma/\rho^{2/3}U_0$ which is the typical time after which a free particle has diffused over its mean-interparticle distance a. The typical size of the time step was $\Delta t=0.003\tau$.

We studied the system as a function of temperature T^*, starting with small temperatures and continuing our simulations by heating the system. The temperature was increased discontinuously in small steps. Between the discontinuous heating process we kept the temperature constant and simulated typically 2×10^4 time steps which correspond to a simulation time of 60τ. After an initial relaxation period of 20τ, statistics were gathered. During the simulations, we monitored the reduced root mean-square displacement (i.e., the Lindemann parameter L) of the particles in order to locate the crystal melting transition. The system either runs in a steady-state situation where the fcc solid remains stable or it suddenly melts at the melting temperature T_m^* losing its crystalline order. The melting process is signaled by a drastic increase of the Lindemann parameter. In fact, after the melting process is finished L grows steadily with simulation time indicating a finite long-time self diffusion in the fluid.

In the equilibrium situation ($p_Z=0$), it is known that rather long simulation runs are needed to obtain the solid melting point precisely. For shorter simulation times one rather probes the spinodal instability of a superheated solid [37] which occurs at higher temperatures. Hence our melting temperature T_m^* is systematically too large. An estimate of the error can be obtained by cooling a molten system. Typically the system exhibits a hysteresis effect. The associated refreezing temperature T_f^* as monitored by a decreasing Lindemann parameter is smaller that the real melting temperature. Hence the real temperature should be in the interval bounded by T_m^* and T_f^*. As we shall demonstrate below, this method gives the melting temperature with a relative error of 5–10 %. It has the advantage that it can be directly applied to a nonequilibrium case where the thermodynamic criteria of phase coexistence are missing.

We finally remark that the system did not refreeze into the initial fcc structure but was rather trapped in an amorphous glass upon cooling. Nevertheless the fcc crystal is the thermodynamic stable state, at least for small polydispersities. Still, as the kinetic glass transition is occurring for smaller temperatures than the recrystallization transition, T_f^* provides a lower bound for the true melting point.

V. RESULTS

In Figs. 1(a)–1(c), the time- and polydispersity-averaged Lindemann parameter $L=\sqrt{\langle\vec{r}_i^2\rangle}/a$ is displayed versus temperature T^*. Clearly, L is increasing with temperature. Figure 1(a) shows the monodisperse case in equilibrium. The arrow indicates the bulk melting point of the Yukawa solid at $T^*\approx0.206$ as obtained by thermodynamic integration [28]. From Fig. 1(a) it becomes clear that our simulation method (data along the dashed line) provides a reasonable estimate of the melting transition. In fact, the equilibrium melting temperature is within the loop resulting from the hystersis by cooling the molten system. Theoretical results for L from our cell model are shown as solid line. As the cell model neglects the mobility of the neighbor cage completely, it is reliable only for small temperatures and underestimates L for larger temperatures. These findings are consistent with our discussion in Sec. III B.

In Fig. 1(b) the equilibrium case for a charge-polydisperse sample is shown. The melting point occurs at $L=0.18$ which is the same value as in the monodisperse case. Again the theory underestimates the Lindemann parameter.

Finally, in Fig. 1(c), a nonequilibrium situation is shown. The melting point in nonequilibrium can be detected by the same analysis as in equilibrium: it is signaled by a dramatic increase of L and the error in locating the melting point can be estimated by cooling the system down again resulting in a narrow hysteresis loop. The Lindemann parameter at melting is again 0.18. The theory underestimates L as in equilibrium.

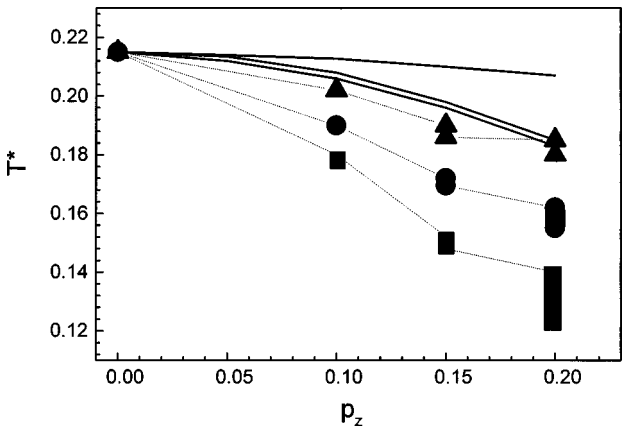

FIG. 2. Melting line away from equilibrium under the influence of an oscillating field as a function of the relative charge polydispersity p_Z and the reduced temperature T^*. λ is fixed to 5.8. The solid lines are from cell theory. The associated three parameter combinations are (i) equilibrium $E_0/k_BT \equiv 0$ (upper curve), (ii) nonequilibrium: $\omega\tau = 1140$ and $E_0/k_BT = 100$, (iii) nonequilibrium: $\omega\tau = 570$ and $E_0/k_BT = 100$ (lowest curve). The symbols show the results of the computer simulation for the same parameter combinations; triangles are for case (i), circles for case (ii), and rectangles for case (iii). The size of the symbols corresponds to the error of the simulation data. The dotted lines are a guide to the eye.

To summarize, one important finding is that the Lindemann parameter at melting was always around 0.18. This was even true for 15 other parameter combinations involving quite different frequencies and field strengths. This implies that the generalization of the Lindemann melting from equilibrium to nonequilibrium is valid, which justifies our basic theoretical assumption.

Several data for melting in nonequilibrium are collected in Fig. 2. We have shown melting lines in the p_Z-T^* plane for three different parameter combinations. The solid lines are obtained from our cell theory. We have matched L_0 to be 0.1028 in order to fix the equilibrium transition for a monodisperse sample at $T^* = 0.21$. Simulation data are shown as symbols. The simulation error as obtained via the width of the corresponding hysteresis loop is indicated by the symbol size. The error becomes larger for large polydispersities which might be due to the fact that the fcc solid is no longer stable. In theory and simulation, the melting line shifts towards smaller temperatures as the polydispersity is increased. The theoretical transition temperatures are, however, systematically too high as compared to the ''exact'' simulation data. This is obviously due to the theoretical assumption that the neighbor cage is completely fixed relative to the overall dynamical mode. This clearly results in a more stable solid and in a higher nonequilibrium melting temperature. Due to the large simulation error, we cannot extract the scaling of the shift from small p_Z definitively, but we can certainly rule out a linear scaling. Hence the p_Z^2 scaling as predicted by cell theory is compatible with our simulation data.

In conclusion, the cell theory is in reasonable but not in full quantitative agreement with the simulation. Still all trends are predicted correctly within the theory.

VI. CONCLUSIONS

In conclusion, we have studied the melting of polydisperse colloidal crystals in an oscillating external field by computer simulation and theory. The simulation data provide compelling evidence that the Lindemann melting rule does also apply in nonequilibrium. The external field shifts the melting point towards lower temperatures. The shift can be understood semiquantitatively within a simple solid cell model of a Brownian oscillator. It scales with the square of the polydispersity.

In fact, it would be interesting to verify our predictions in experiments on real colloidal samples. Different realizations of such an external field as oscillatory shear and external laser-optical or magnetic fields are conceivable. If the melting point is known in a sensible experiment by a suitable gauging, the shift of the melting line gives direct information about the intrinsic polydispersity of the colloidal suspensions.

We finish with a couple of remarks and state some interesting open questions: First, one should develop — with the help of the Smoluchowski equation — a density functional theory of freezing [2] away from equilibrium. Second, a binary solid should be investigated in more detail. For large asymmetries of the two particle species, the external field may induce a phase separation from a random-occupied crystal into two single crystals occupied by only one of the two species. Third, in noncubic crystals the shift will also depend strongly on the orientation of the external field. It would be interesting to study how this anisotropy affects the melting point. Finally, the nonequilibrium molten state should be investigated in more detail: its anisotropic structural correlations in a steady state should be compared to the equilibrium correlations. Here further data from computer simulations as well as the development of liquid integral equations [38] in nonequilibrium are highly desirable. Even in the liquid phase there might be a further phase transformation into a structured liquid with separated stripes of high-charge and low-charge colloidal particles.

As discussed in Sec. II, the melting transition of a monodisperse colloidal system exhibiting simple Brownian dynamics without any hydrodynamic interactions is not affected at all by a space-independent oscillating field. The present paper discusses a nontrivial model by considering polydisperse samples. There are two other situations for a monodisperse system where the space-independent oscillating field has a nontrivial influence on melting. If inertia effects are incorporated in the dynamics, our general argument for a dynamical overall mode does not hold. This applies, e.g., for Fokker-Planck dynamics which can be used as a description for the dynamics of dusty plasmas [39]. Second a serious complication arises if hydrodynamic interactions [40,41] are taken into account. Then the field will have an influence on the melting line for a monodisperse sample. Both cases should be explored in more detail in future studies.

ACKNOWLEDGMENTS

We thank M. Schmidt, M. Watzlawek, J. K. G. Dhont, and G. Nägele for helpful remarks.

[1] *Observation, Prediction and Simulation of Phase Transitions in Complex Fluids, Series C*, edited by M. Baus, L. F. Rull, and J. P. Ryckaert (Kluwer Academic Publishers, Dordrecht, 1995), Vol. 460.
[2] H. Löwen, Phys. Rep. **237**, 249 (1994).
[3] W. Ostwald, Z. Phys. Chem. **22**, 289 (1897).
[4] J. Bechhoefer, H. Löwen, and L. Tuckerman, Phys. Rev. Lett. **67**, 1266 (1991).
[5] For a review, see P. N. Pusey, in *Liquids, Freezing and the Glass Transition*, edited by J. P. Hansen, D. Levesque, and J. Zinn-Justing (North-Holland, Amsterdam, 1991).
[6] A. K. Arora and B. V. R. Tata, Adv. Colloid Interface Sci. **78**, 49 (1998).
[7] T. Palberg, W. Mönch, J. Schwarz, and P. Leiderer, J. Chem. Phys. **102**, 5082 (1995).
[8] A. Chowdhury, B. J. Ackerson, and N. A. Clark, Phys. Rev. Lett. **55**, 833 (1985); A. P. Gast and C. F. Zukowski, Adv. Colloid Interface Sci. **30**, 153 (1989); R. Kesavamoorthy, R. Jagannathan, S. Rundquist, and S. A. Asher, J. Chem. Phys. **94**, 5172 (1991).
[9] A. T. Skeltrop, J. Appl. Phys. **55**, 2587 (1984).
[10] For a review see A. Onuki, J. Phys.: Condens. Matter **9**, 6119 (1997).
[11] R. Lahiri and S. Ramaswamy, Physica A **224**, 84 (1996).
[12] As for recent computer simulation studies, see, M. J. Stevens and M. O. Robbins, Phys. Rev. E **48**, 3778 (1993); S. Butler and P. Harrowell, J. Chem. Phys. **103**, 4653 (1995); S. R. Rastogi, N. J. Wagner, and S. R. Lustig, *ibid.* **104**, 9234 (1996); J. F. Lutsko, Phys. Rev. Lett. **77**, 2225 (1996); E. S. Boek, P. V. Coveney, H. N. W. Lekkerkerker, and P. van der Schoot, Phys. Rev. E **55**, 3124 (1997); N. Olivi-Tran, R. Botet, and B. Cabane, Phys. Rev. E **57**, 1997 (1998).
[13] B. J. Ackerson and P. N. Pusey, Phys. Rev. Lett. **61**, 1033 (1988).
[14] Y. D. Yan, J. K. G. Dhont, C. Smits, and H. N. W. Lekkerkerker, Physica A **202**, 68 (1994).
[15] W. Xue and G. S. Grest, Phys. Rev. Lett. **64**, 419 (1990); H. Komatsugawa and S. Nosé, Phys. Rev. E **51**, 5944 (1995); **53**, 2588 (1996); S. Butler and P. Harrowell, J. Chem. Phys. **105**, 605 (1996).
[16] G. K. Batchelor, J. Fluid Mech. **119**, 379 (1982); G. K. Batchelor, C.-S. Wen, *ibid.* **124**, 495 (1982).
[17] R. Lahiri and S. Ramaswamy, Phys. Rev. Lett. **79**, 1150 (1997).
[18] T. Palberg, R. Simon, M. Würth, and P. Leiderer, Prog. Colloid Polym. Sci. **96**, 62 (1994).
[19] H. Löwen, J. N. Roux, and J. P. Hansen, Phys. Rev. A **44**, 1169 (1991); H. Löwen, J. P. Hansen, and J. N. Roux, J. Phys.: Condens. Matter **3**, 997 (1991).
[20] B. D'Aguanno and R. Klein, J. Chem. Soc., Faraday Trans. **87**, 379 (1991); Phys. Rev. A **46**, 7652 (1992).
[21] One should bear in mind, however, that counterion friction effects may also become important, see, e.g., K. Schtäzel, W. Weise, A. Sobotta, and M. Drewel, J. Colloid Interface Sci. **143**, 287 (1991); T. Palberg, M. Evers, N. Garbow, and D. Hessinger, in *Transport and Structure in Biophysical and Chemical Phenomena*, edited by S. C. Muller, J. Parisi, and W. Zimmerman (Springer, New York, in press).
[22] The same conclusion can be drawn from the equivalent Smoluchowski picture by changing variables appropriately in the Smoluchowski equation.
[23] R. Piazza and V. Degiorgio, Physica A **182**, 576 (1992).
[24] F. A. Lindemann, Phys. Z. **11**, 609 (1910).
[25] H. Löwen, T. Palberg, and R. Simon, Phys. Rev. Lett. **70**, 1557 (1993).
[26] R. Ohnesorge, H. Löwen, and H. Wagner, Europhys. Lett. **22**, 245 (1993).
[27] M. O. Robbins, K. Kremer, and G. S. Grest, J. Chem. Phys. **88**, 3286 (1988).
[28] E. J. Meijer and D. Frenkel, J. Chem. Phys. **94**, 2269 (1991).
[29] M. J. Stevens and M. O. Robbins, J. Chem. Phys. **98**, 2319 (1993).
[30] S.-E. Phan, W. B. Russel, J. Zhu, and P. M. Chaikin, J. Chem. Phys. **108**, 9789 (1998).
[31] B. V. R. Tata and A. K. Arora, J. Phys.: Condens. Matter **3**, 7983 (1991).
[32] P. G. Bolhuis and D. A. Kofke, J. Phys.: Condens. Matter **8**, 9627 (1996); Phys. Rev. E **54**, 634 (1996).
[33] P. Bartlett, J. Chem. Phys. **109**, 10 970 (1998).
[34] D. A. Kofke, P. G. Bolhuis, Phys. Rev. E **59**, 618 (1999).
[35] D. L. Ermak, J. Chem. Phys. **62**, 4189 (1975); **62**, 4197 (1975).
[36] See, e.g., M. P. Allen and D. J. Tildesley, *Computer Simulation of Liquids* (Clarendon Press, Oxford, 1989).
[37] R. M. J. Cotterhill, W. D. Kristensen, and E. J. Jensen, Philos. Mag. **31**, 245 (1974).
[38] See, e.g., J. P. Hansen and I. R. McDonald, *Theory of Simple Liquids*, 2nd ed. (Academic, London, 1986).
[39] M. Zuzic, H. M. Thomas, and G. E. Morfill, J. Vac. Sci. Technol. A **14**, 496 (1996); V. A. Schweigert, I. V. Schweigert, A. Melzer, A. Homann, and A. Piel, Phys. Rev. Lett. **80**, 5345 (1998).
[40] G. Nägele, Phys. Rep. **272**, 215 (1996).
[41] J. K. G. Dhont, *An Introduction to Dynamics of Colloids* (Elsevier, Amsterdam, 1996).